Università degli Studi di Padova

Dipartimento di Scienze Chimiche
Università degli Studi di Padova
via Marzolo 1, 35131 Padova Italy

Multidimensional and Ultrafast Optical Spectroscopy Group

Coherent multidimensional spectroscopies: advanced spectroscopic techniques to unveil complex dynamics

Elisabetta Collini
elisabetta.collini@unipd.it

keywords

‘coherent’

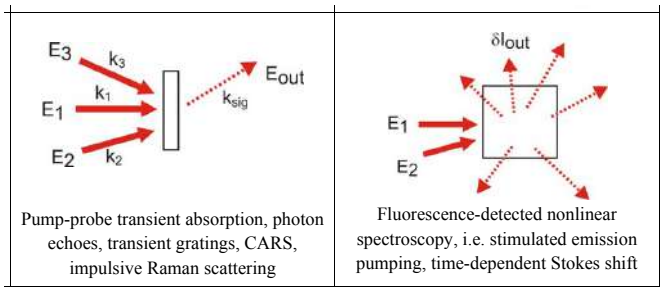

Pump-probe transient absorption, photon echoes, transient gratings, CARS, impulsive Raman scattering

Fluorescence-detected nonlinear spectroscopy, i.e. stimulated emission pumping, time-dependent Stokes shift

‘multidimensional’

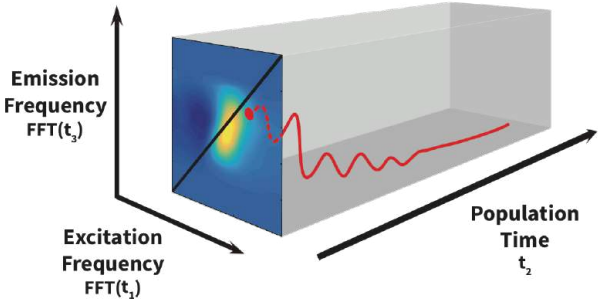

‘dynamics’

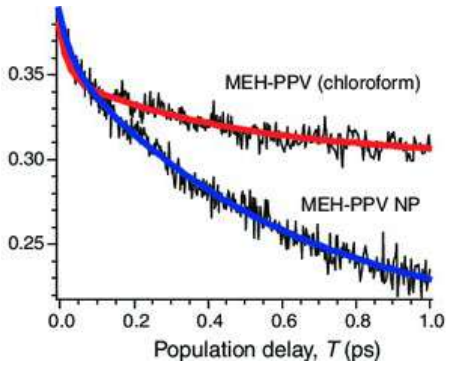

‘complex’

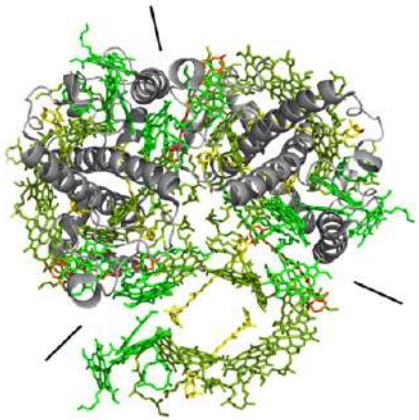

historical overview

A second dimension was introduced for the first time in NMR spectroscopy,
NOESY (nuclear Overhauser enhancement spectroscopy)
COSY (correlation spectroscopy)
These technique have been extensively used to study structural and dynamical properties of proteins in solution.

2D-NMR 1970

In the optical regime, the origin of multidimensional vibrational spectroscopy can be traced to the coherent anti-Stokes Raman spectroscopy (CARS) measurements of vibrational dephasing performed in the 1970s.
2D vibrational spectroscopic technique (2D-IR) can provide detailed information on the 3D structure of a given complex molecule, i.e., proteins, water networks,…

2D-IR 1980-90

2D electronic spectroscopy was introduced by Fleming
Delay with respect to the IR counterpart due to experimental problems connected with the higher frequency of Visible light.

2D-ES 2000

CMDS @ the third order: 2DES

CMDS techniques can be declined at different orders of the nonlinear polarizability (3° , 5° , etc.) and in different spectral ranges (IR, Vis, UV…)

2D electronic spectroscopy:

- third order technique: generalized version of a 4-wave mixing spectroscopy
- in the Vis range: electronic transitions

2D electronic spectroscopy (2DES): why and when?

from 1D to 2D

Conventional optical spectroscopy techniques, such as ordinary infrared, Raman, and UV-visible spectroscopies, provide a one dimensional (1D) projection of the available molecular information of a sample onto a single frequency axis. In contrast, optical multidimensional (2D, 3D) spectroscopy techniques provide a multidimensional projection of the relevant molecular motions offering dramatically more information.

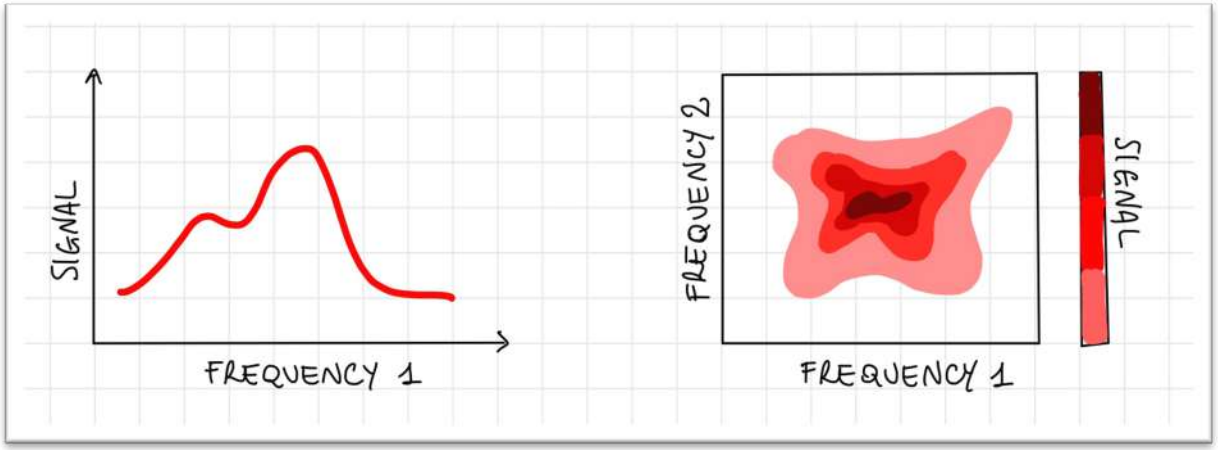

why 2DES ?

NUMBER OF OBSERVABLES (PEAKS)
~ N (1D)
~ N^2 (2D)
~ N^d (d-dimensional spectroscopy)

- Spread information along multiple dimensions
- Simultaneously frequency and time-resolved
- Couplings and transport processes mapped far from diagonal positions (where main dynamical processes take place)
- Sensitivity to coherent dynamic mechanisms (oscillations)

Why not?

- complex (and expensive) optical setups
- demanding data processing and analysis
- challenging interpretation of the data (artefacts)

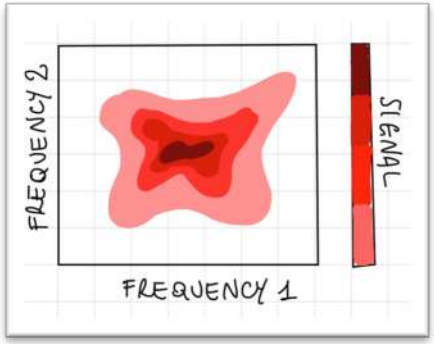

ideal to untangle complex dynamics (transport processes)
in complex multichromophore systems

biological antennas

JPCLett11(2020)1059
NatureComm9(2018)3160

JPCLett11(2020)7972

porphyrin-peptide self assemblies

PCCP22(2020)7516

rhodamine dimers on DNA

Nanoscale(2021)
10.1039/D1NR00775K

hybrid metal-organic nanomaterials

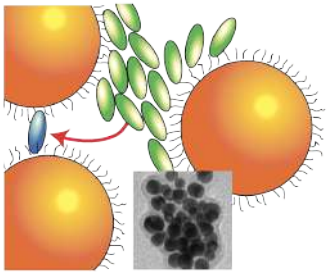

JPCLett7(2016)4996

strongly coupled J-aggregates

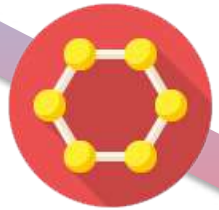

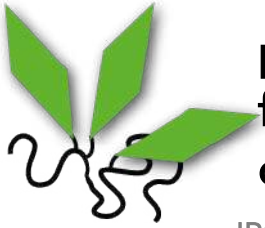

porphyrin functionalized oligomers

JPCC123(2019)10212

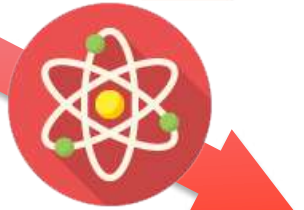

transport in QDs materials

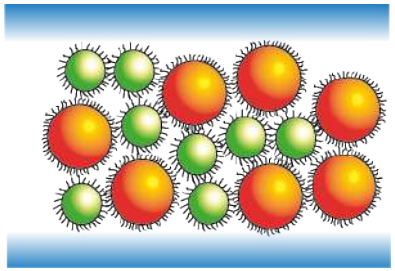

JPCC124(2020)16222
JPCC123(2019)31286
JCP154(2021)014301

2D electronic spectroscopy: the experiment

2DES setup

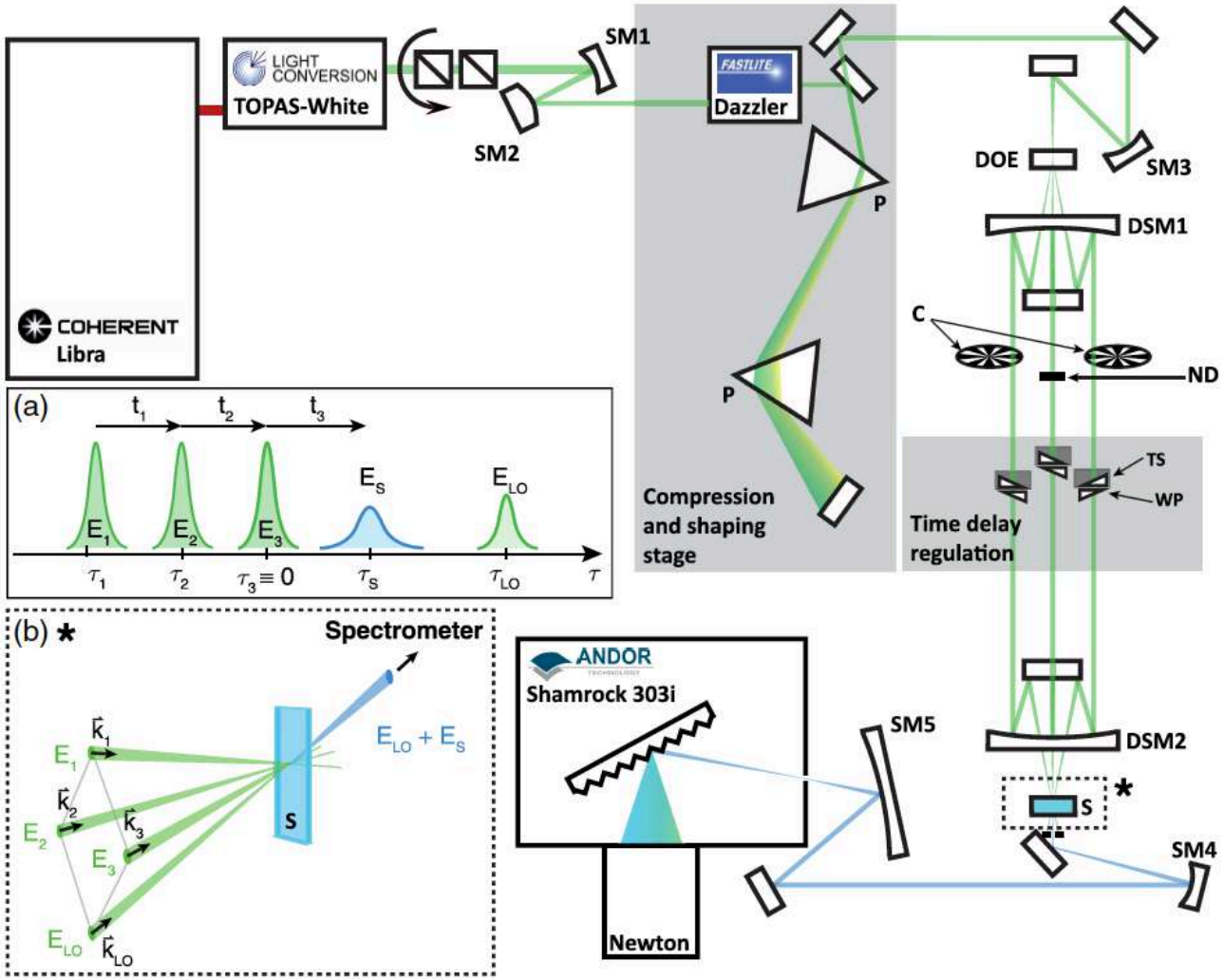

JOSAB 34(2017)1223

Heterodyne detection

$$I_{\mathrm{det},HOMO} = \frac{nc}{8\pi}\left|E_S\right|^2 \qquad I_{\mathrm{det},HET} = \frac{n(\omega_S)c}{4\pi}\left|E_{LO}(t)+E_S(t)\right|^2 =$$

$$= I_{LO} + I_S + 2\frac{n(\omega_S)c}{4\pi}\mathrm{Re}\left[E_{LO}^*(t)\cdot E_S(t)\right]$$

The heterodyne signal is linear rather than quadratic in the (weak) signal field

By controlling the relative phase of E_{LO} and E_S it is possible to probe separately the real and imaginary part ⇒ *phase sensitive detection*

interferogram

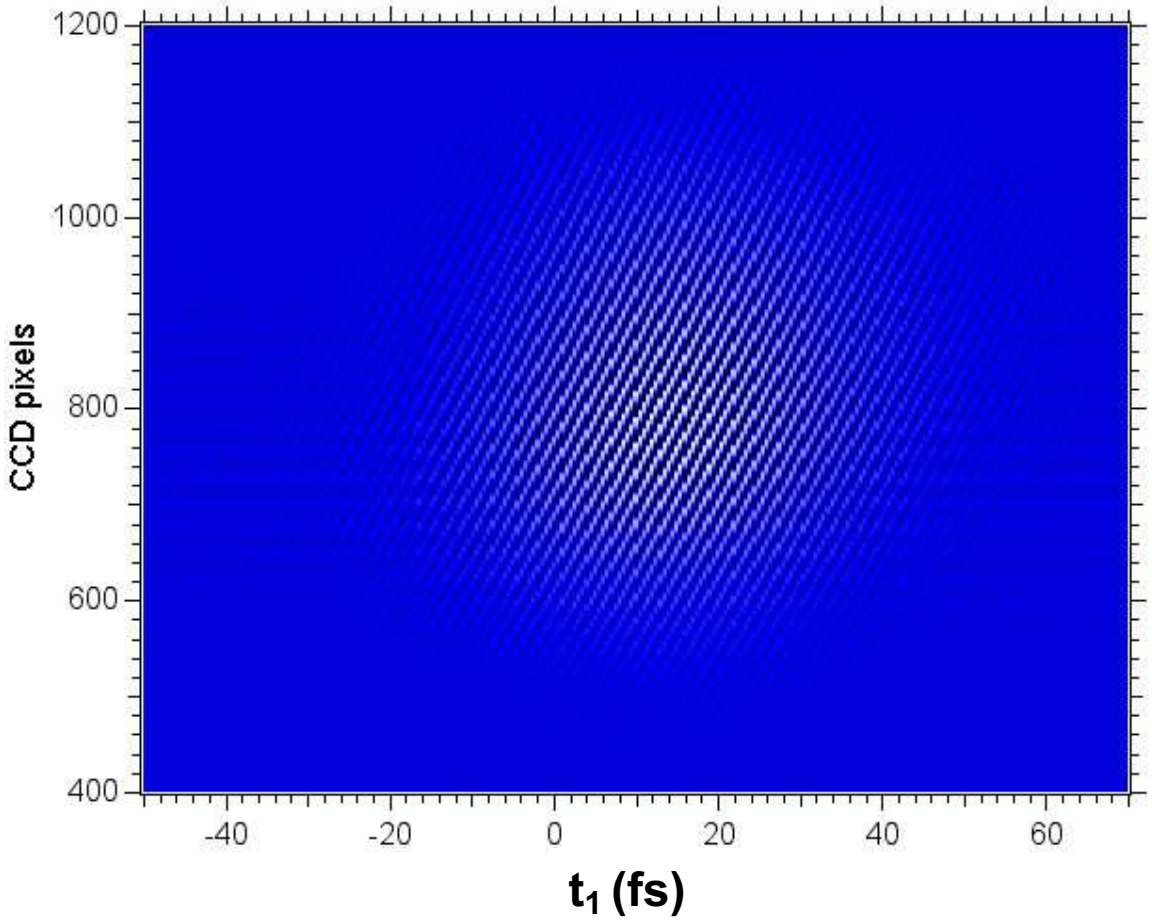

From interferograms to 2D spectra

$$I(\omega) = 2\mathrm{Re}\left[E^*_{LO}(\omega)\cdot E_S(\omega)\cdot e^{-i\omega\Delta\tau}\right]$$

$$E_S(\omega) = \frac{FFT\left[\theta(t)\, IFFT\left\{I(\omega)\right\}\right]e^{-i\omega\Delta\tau}}{E^*_{LO}(\omega)}$$

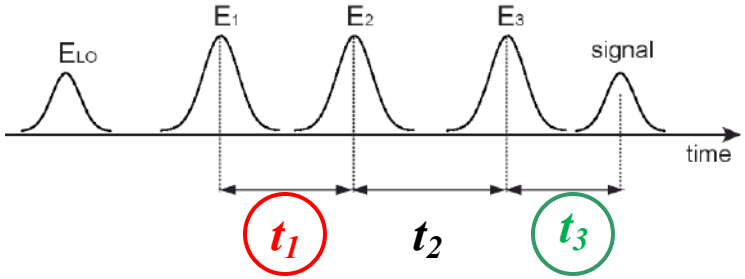

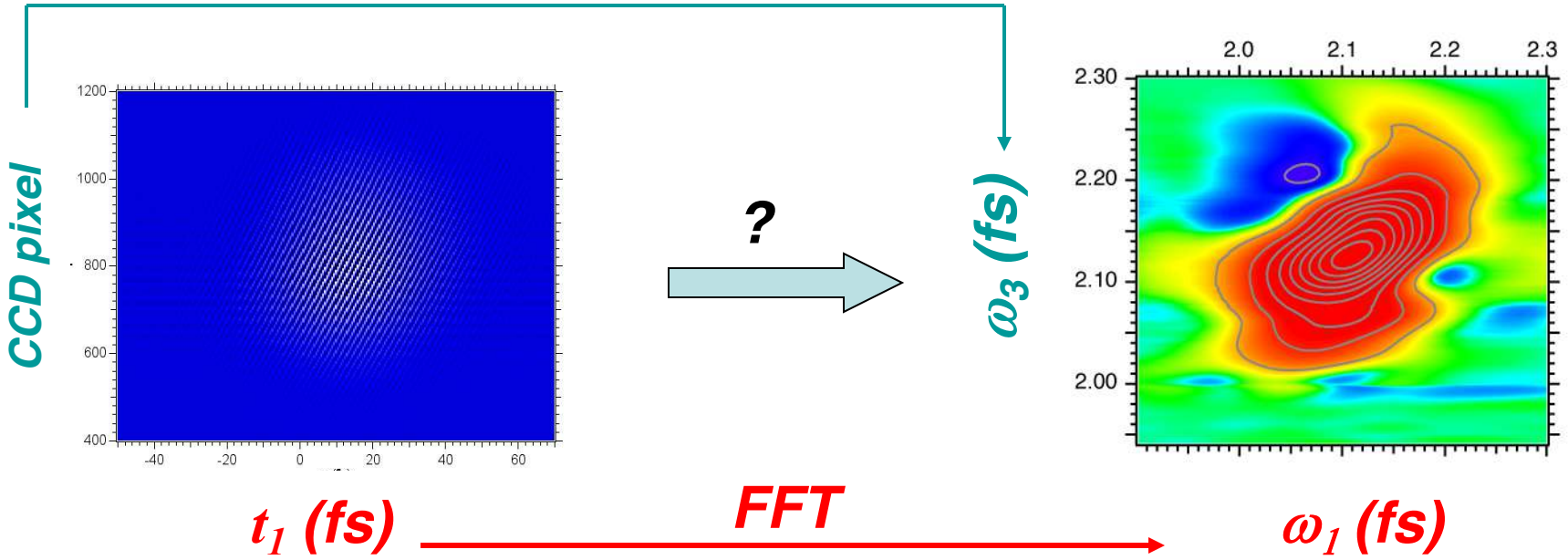

From interferograms to 2D spectra

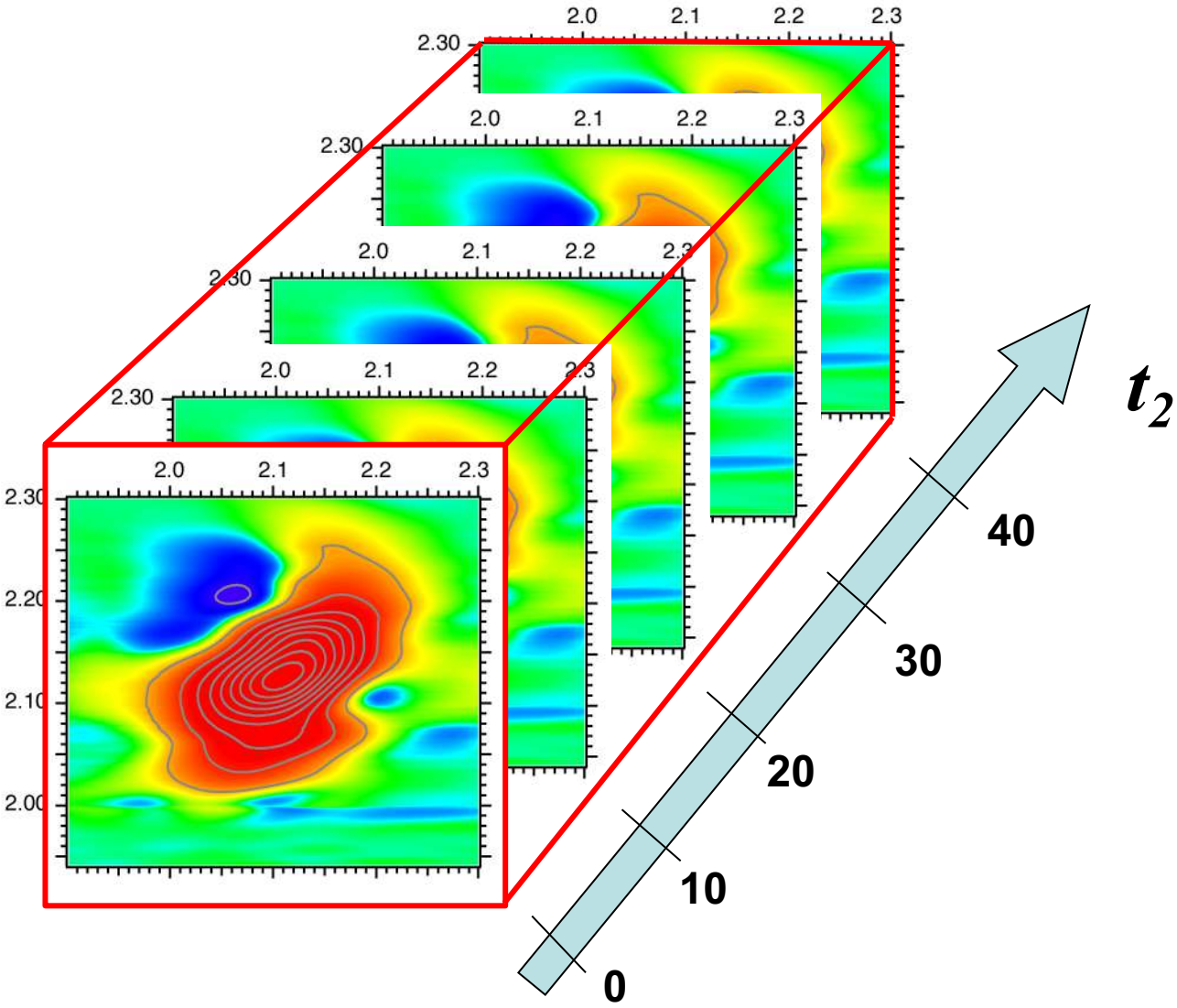

Response Function Formalism

time-resolved non-linear techniques

Time-resolved techniques

In the **perturbative approach**, the signal is proportional to the polarization $P(r,t)$, induced in the sample by the interaction with electric fields, expressed as convolution between the fields and with the molecular response function $R^{(n)}$:

$$P_i^{(n)}(t) = \int_{-\infty}^{+\infty}\int_{-\infty}^{+\infty}\dots\int_{-\infty}^{+\infty} dt_1\, dt_2 \dots dt_n R^{(n)}_{ijk\dots l}(t-t_1, t-t_2, \dots, t-t_n) \times$$

$$E_j(t_1)E_k(t_2)\dots E_l(t_n)$$

S.Mukamel, 'Principles of nonlinear optical spectroscopy'

response function *vs* susceptibility

$$P_i^{(n)}(t) = \int_{-\infty}^{+\infty}\int_{-\infty}^{+\infty}\ldots\int_{-\infty}^{+\infty} d\omega_1\, d\omega_2 \ldots d\omega_n \chi_{ijk\ldots l}^{(n)}(\omega_1,\omega_2,\ldots,\omega_n)\times$$

$$E_j(\omega_1)E_k(\omega_2)\ldots E_l(\omega_n)\exp\left[-i\left(\omega_1+\omega_2+\ldots+\omega_n\right)t\right]$$

$$\chi^{(n)}(\omega_1\cdots\omega_n) = \int_{-\infty}^{+\infty}\cdots\int_{-\infty}^{+\infty} dt_1\cdots dt_n R_i^{(n)}(t_1\cdots t_n)\exp\left(-i\sum_{j=1}^{n}\omega_j t_j\right)$$

The susceptibility $\chi^{(n)}(\omega_1\cdots\omega_n)$ is the **Fourier-Laplace transform** of the response function $R_i^{(n)}(t_1\cdots t_n)$

4-wave mixing: overview

The most general time-resolved experiment related to $P^{(3)}$ requires the interaction with 3 fields and it can be generally indicated as **four wave mixing**.
In the impulsive limit (very short pulses) the signal is directly related to the response function $R^{(3)}$.
It is possible to change the relative time ordering and the phase-matching of the 3 interactions: in this way the signal becomes sensitive only to specific processes, and different techniques may be distinguished (pump&probe, photon echo, transient grating, hole burning,…)

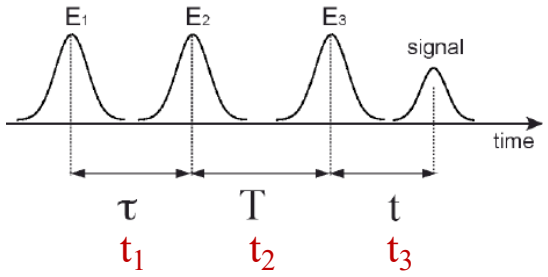

$$P_i^{(3)}(t) = \int_{-\infty}^{+\infty}\int_{-\infty}^{+\infty}\int_{-\infty}^{+\infty} dt_1\, dt_2\, dt_3 R_{ijk}^{(3)}(t-t_1, t-t_2, t-t_3) \times E_1(t_1)E_2(t_2)E_3(t_3)$$

4-wave mixing: overview

$$R^{(3)}_{ijk}(t-t_1,t-t_2,t-t_3)=\sum_{\alpha}R^{(3)}_{\alpha}(t-t_1,t-t_2,t-t_3)$$

$R^{(3)}$ can be calculated within the **perturbation theory** framework using **Feynmann diagrams**. Depending on the pulse order and on the phase matching conditions, only selected diagrams (=evolution pathways along the **density matrix**) will be relevant and this simplify the calculation of the signal.

density matrix

$$\rho(t)\equiv|\psi(t)\rangle\langle\psi(t)|.$$

$$\langle A\rangle=\langle\psi|A|\psi\rangle=Tr[A\rho].$$

— ***b***

— ***a***

$$\begin{bmatrix}\boldsymbol{\rho_{aa}} & \boldsymbol{\rho_{ab}}\\ \boldsymbol{\rho_{ba}} & \boldsymbol{\rho_{bb}}\end{bmatrix}$$

$\begin{bmatrix}\mathbf{1} & \mathbf{0}\\ \mathbf{0} & \mathbf{0}\end{bmatrix}$ The system is described by ψ_a (only the ***a*** state is populated)

$\begin{bmatrix}\frac{\mathbf{1}}{\mathbf{2}} & \frac{\mathbf{1}}{\mathbf{2}}\\ \frac{\mathbf{1}}{\mathbf{2}} & \frac{\mathbf{1}}{\mathbf{2}}\end{bmatrix}$ The system is described by a coherent superposition of ***a*** and ***b*** states: $\frac{1}{2}\psi_a+\frac{1}{2}\psi_b$

diagrams

Feynman diagram

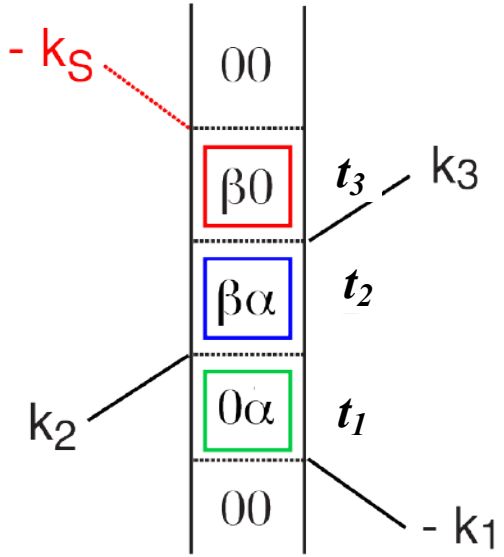

Liouville diagram

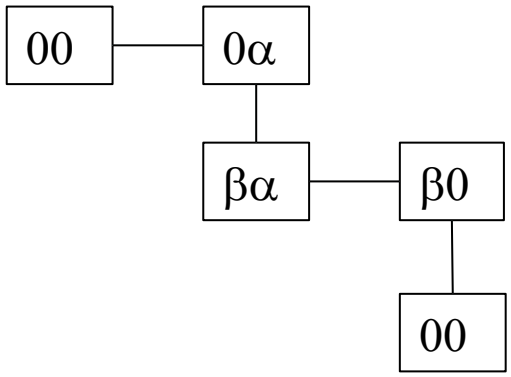

levels diagram

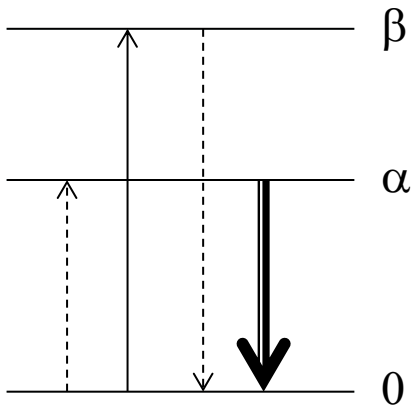

signal, response functions and evolution pathways

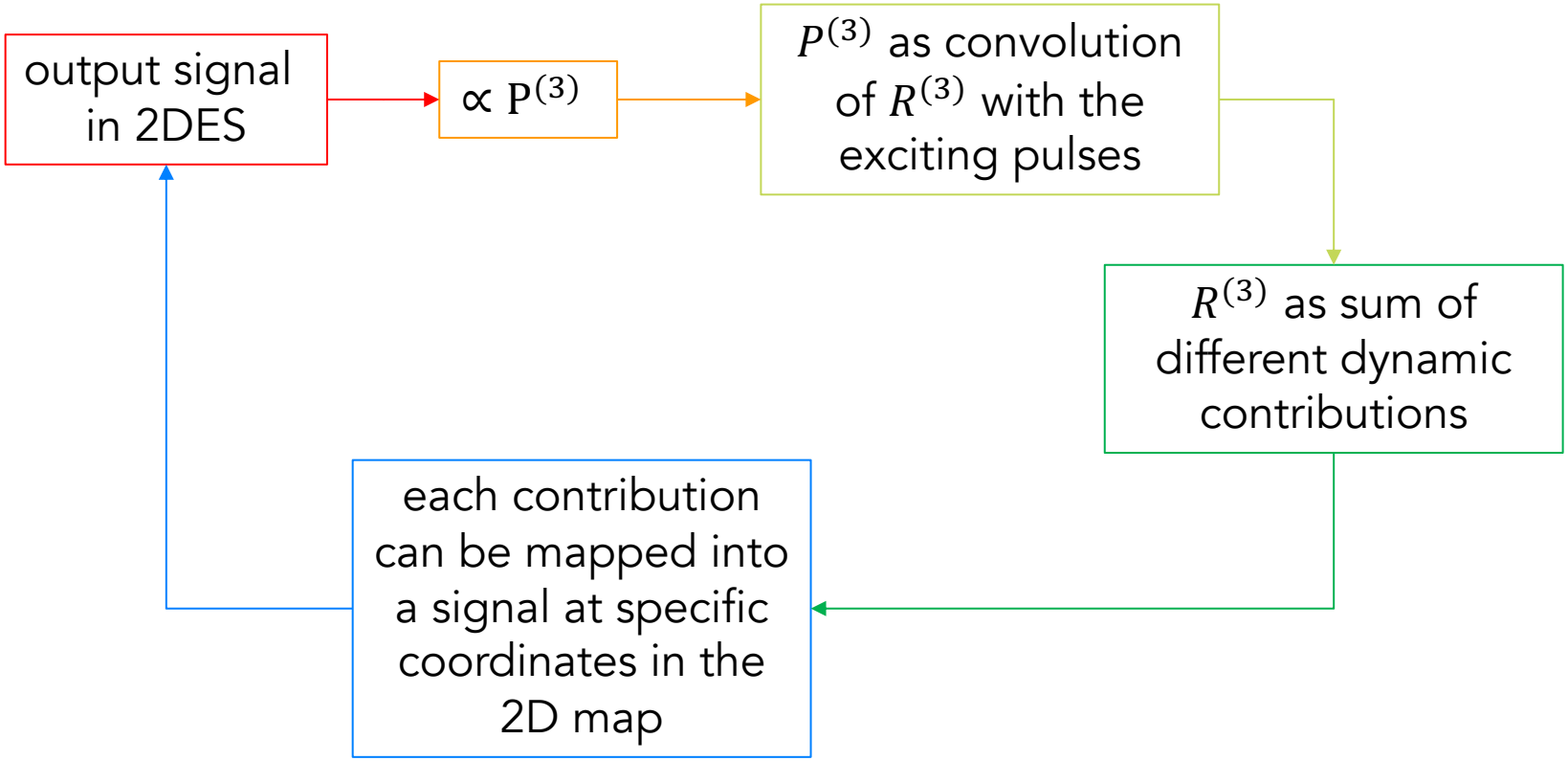

S.Mukamel, 'Principles of nonlinear optical spectroscopy', 1995
A.Tokmakoff, Time-dependent quantum mechanics and spectroscopy, 2014

2D electronic spectroscopy: qualitative description of the response

2DES: off-diagonal cross-peaks resolve couplings between states

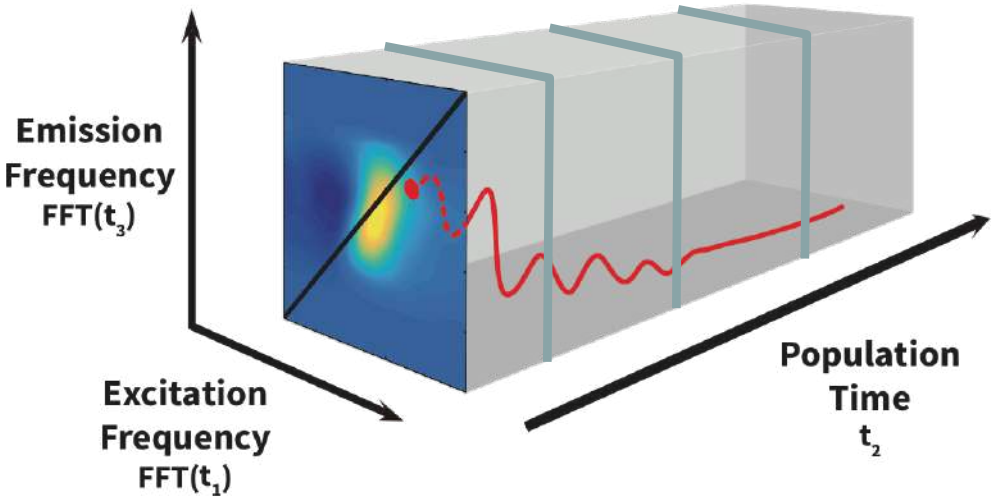

2D maps

@ a fixed value of t_2

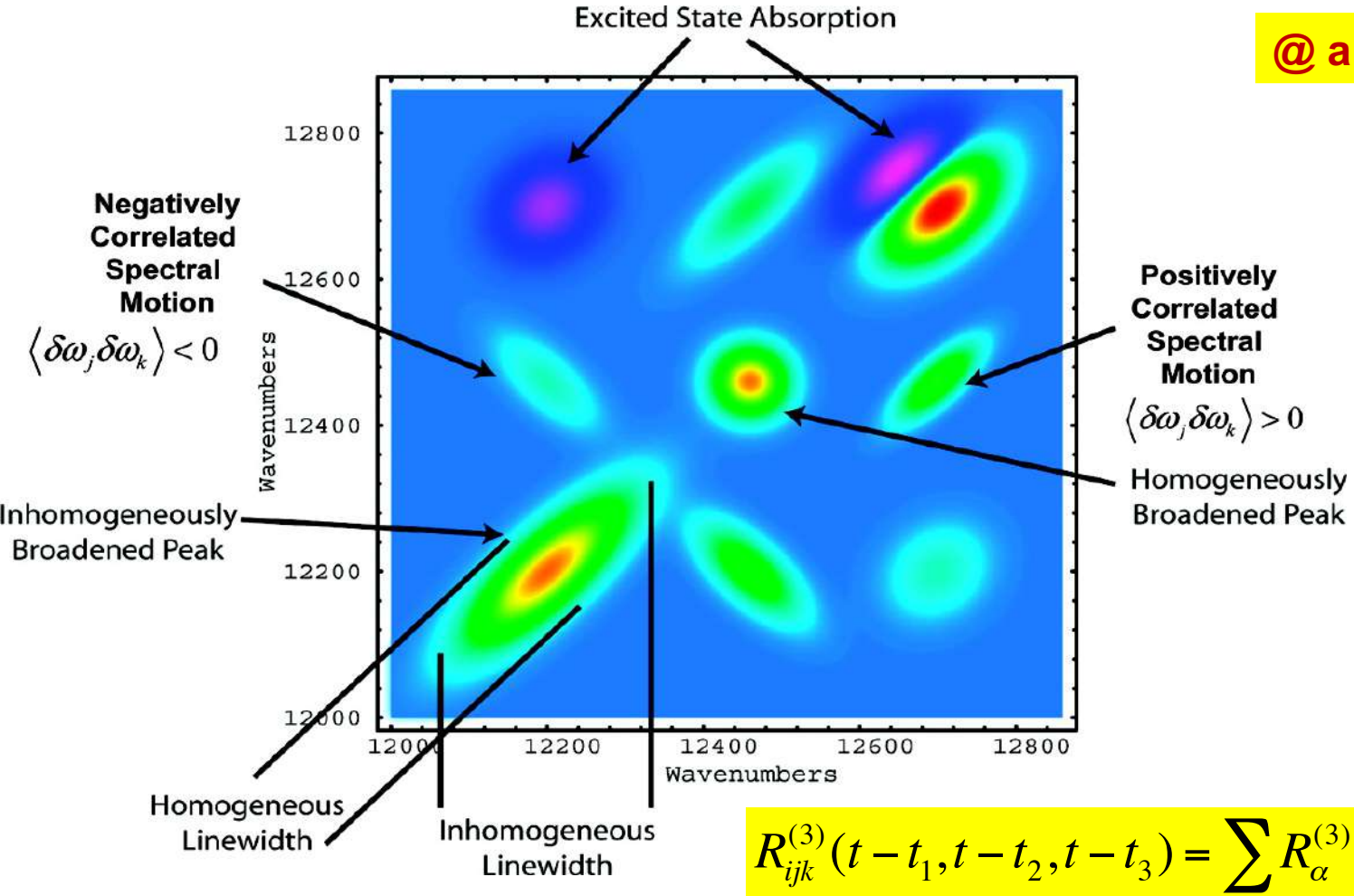

$$R_{ijk}^{(3)}(t-t_1,t-t_2,t-t_3) = \sum_{\alpha} R_{\alpha}^{(3)}(t-t_1,t-t_2,t-t_3)$$

Published in: Minhaeng Cho; Chem. Rev. 2008, 108, 1331-1418.
DOI: 10.1021/cr078377b, Copyright © 2008 American Chemical Society

2DES: off-diagonal cross-peaks resolve couplings between states

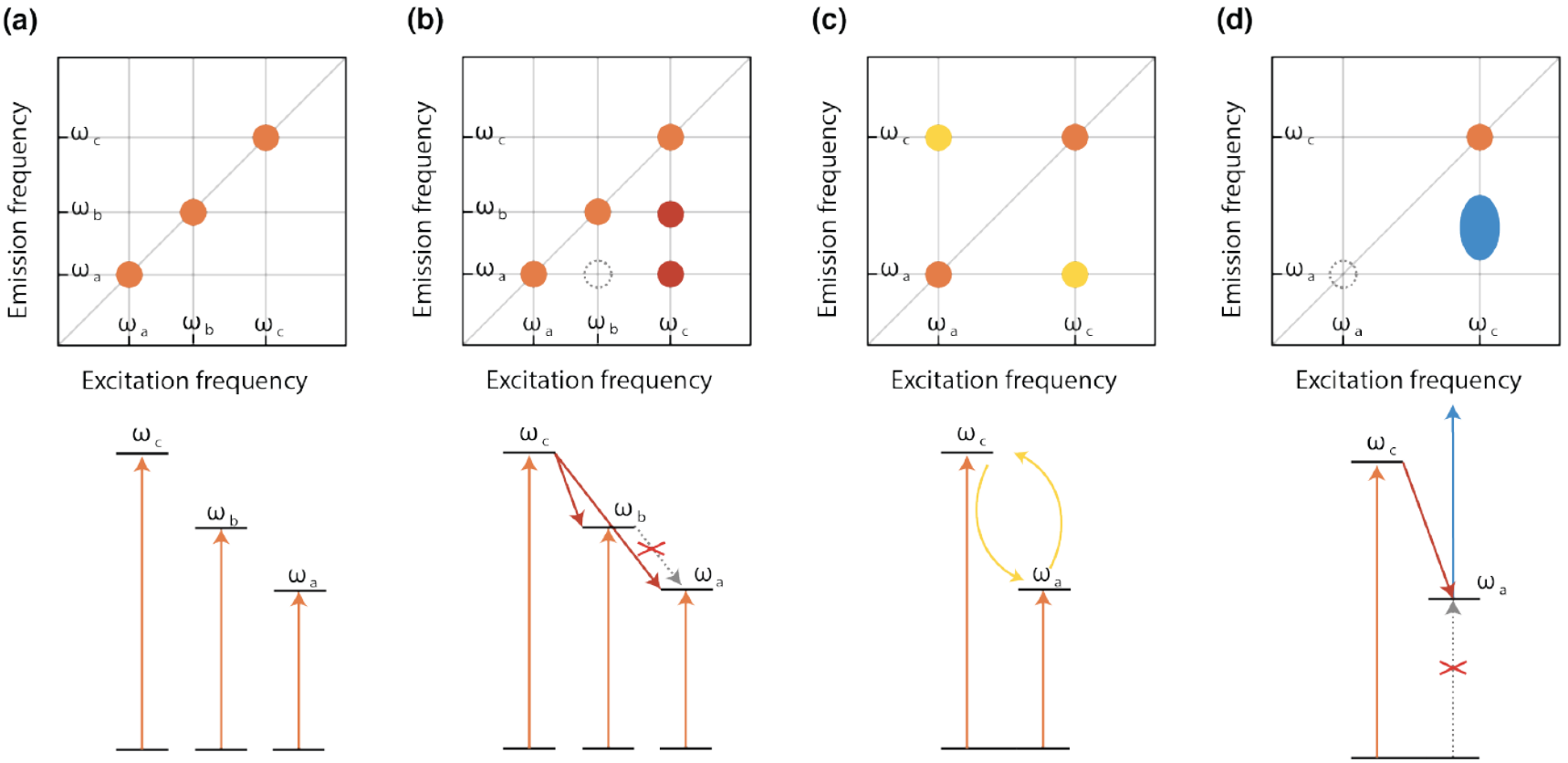

Biochimica et Biophysica Acta 1860 (2019) 271

2DES: off-diagonal cross-peaks resolve couplings between states

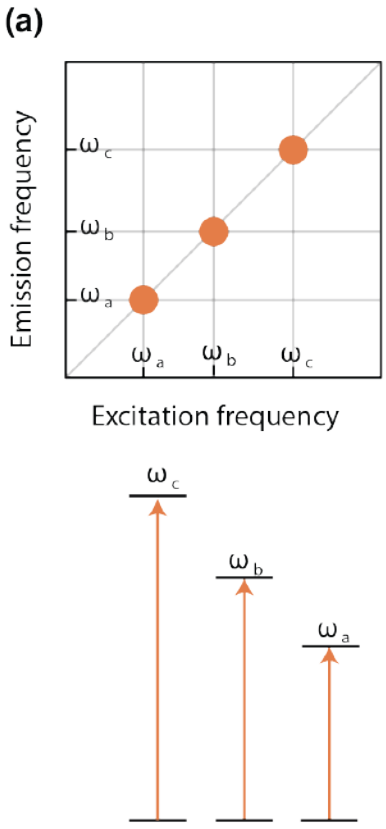

A system that produces multiple diagonal peaks but no cross-peaks can be modeled as a set of isolated non-interacting two-level systems.

2DES: off-diagonal cross-peaks resolve couplings between states

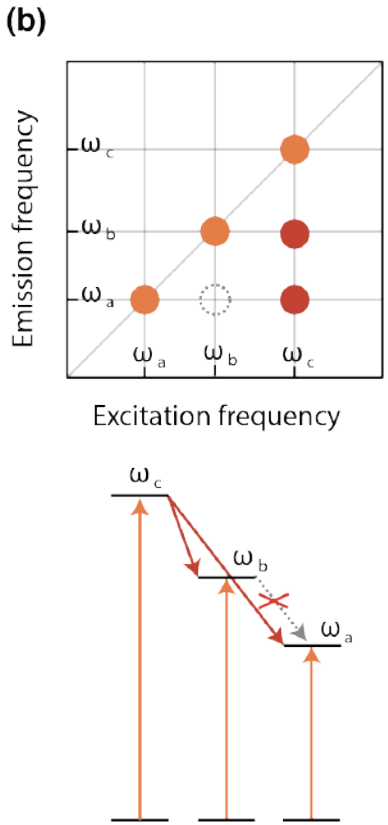

The cross-peaks at coordinates ($\boldsymbol{\omega}_c$, $\boldsymbol{\omega}_b$) and ($\boldsymbol{\omega}_c$, $\boldsymbol{\omega}_a$) appearing at $t_2>0$ indicate that state ***c*** is coupled *via* energy transfer with states ***a*** and ***b*** (Forster energy transfer, FRET).
No coupling between states ***a*** and ***b*** because no cross peak appears at ($\boldsymbol{\omega}_b$, $\boldsymbol{\omega}_a$).

Biochimica et Biophysica Acta 1860 (2019) 271

2DES: off-diagonal cross-peaks resolve couplings between states

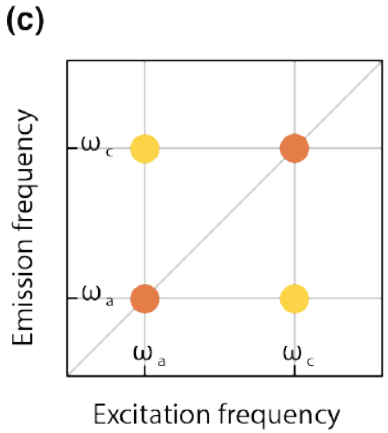

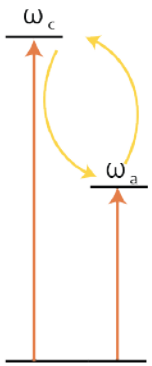

In the presence of resonance interactions between the two states, symmetric above and below diagonal cross-peaks appear already at t_2=0: the system can be modeled as a molecular (excitonic) dimer.

Biochimica et Biophysica Acta 1860 (2019) 271

2DES: off-diagonal cross-peaks resolve couplings between states

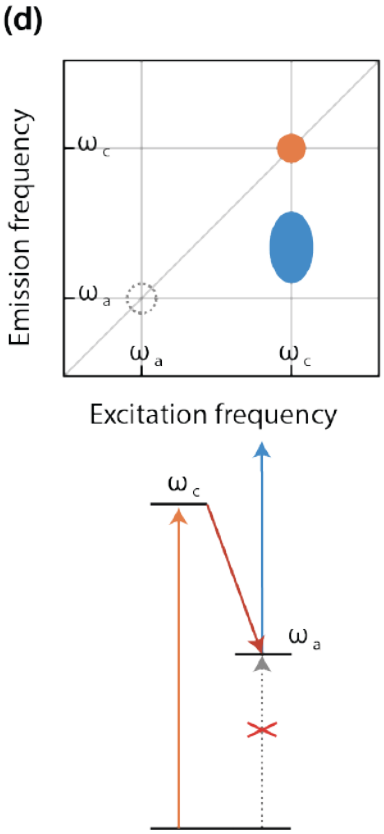

A dark state (ω_a) can be characterized by the coupling with a bright state (ω_c) in excited state absorption processes.

Biochimica et Biophysica Acta 1860 (2019) 271

2D maps (1)

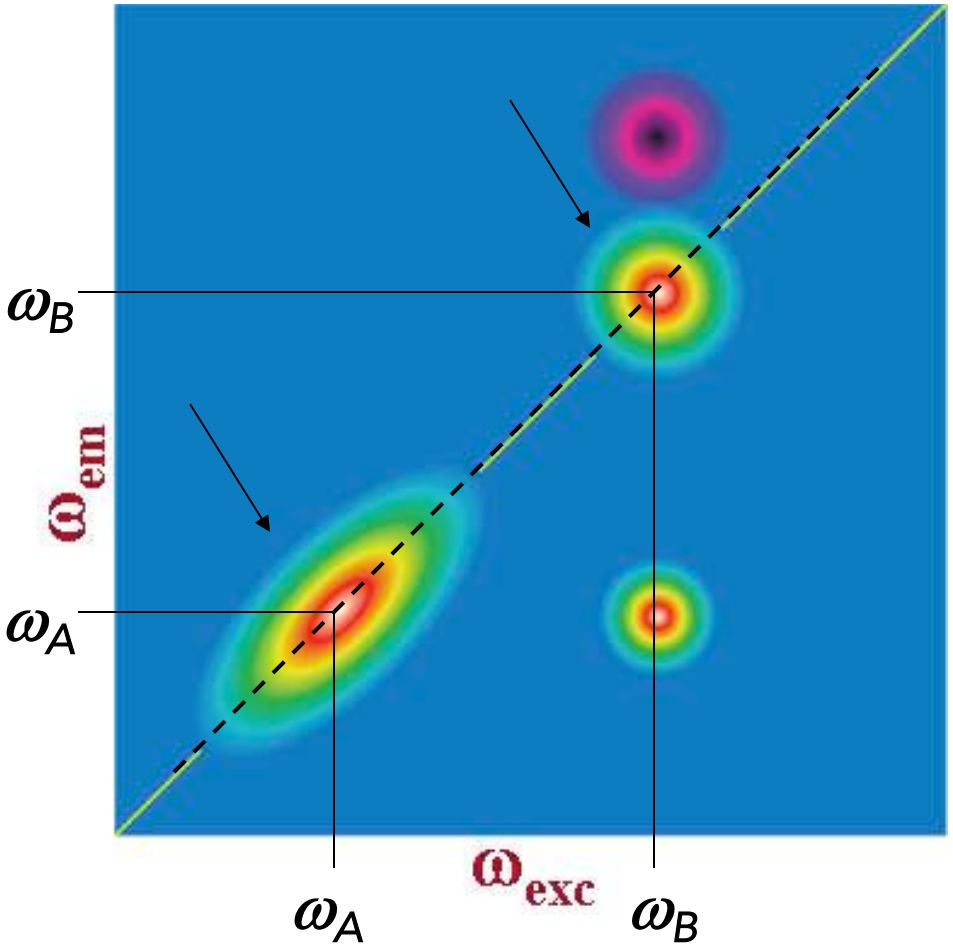

The diagonal section corresponds to linear spectrum.

diagonal peaks
⇓
absorption peaks

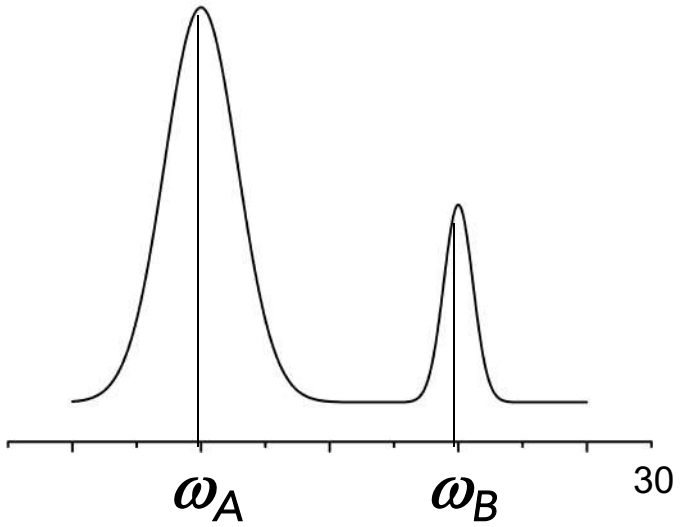

2D maps (2)

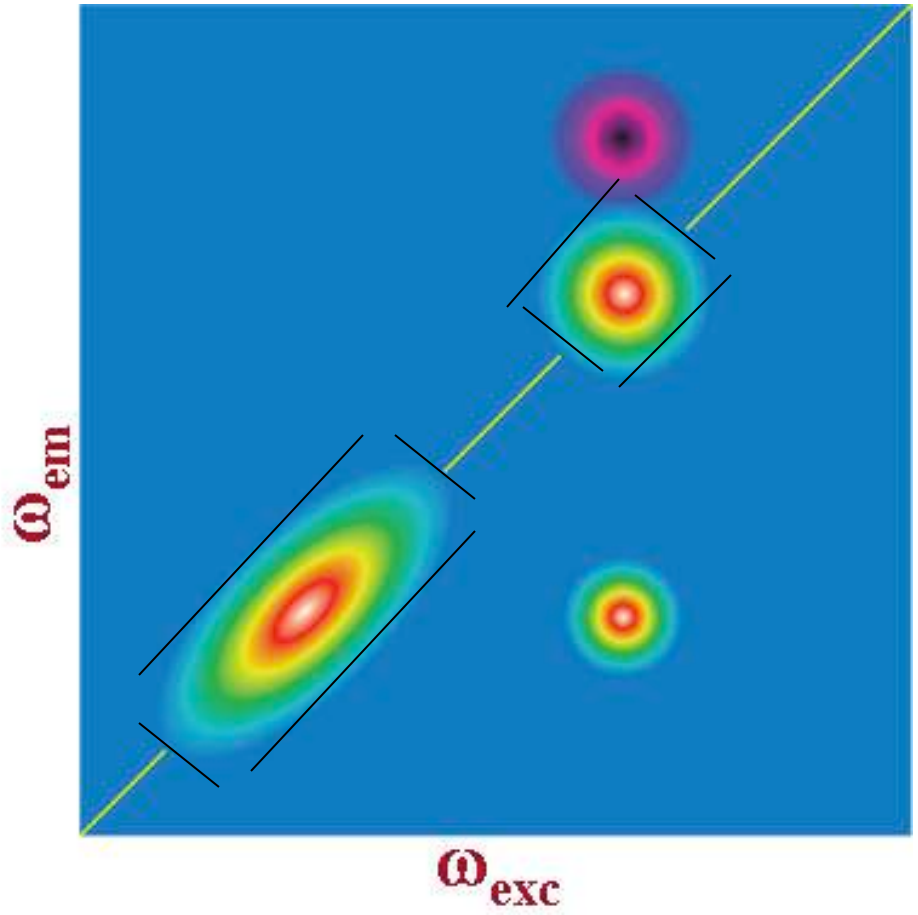

Shape of the 2D spectrum reveals distribution of the environments.

Inhomogeneous broadening: diagonal peak width

Homogeneous width: anti-diagonal peak width

2D maps (3)

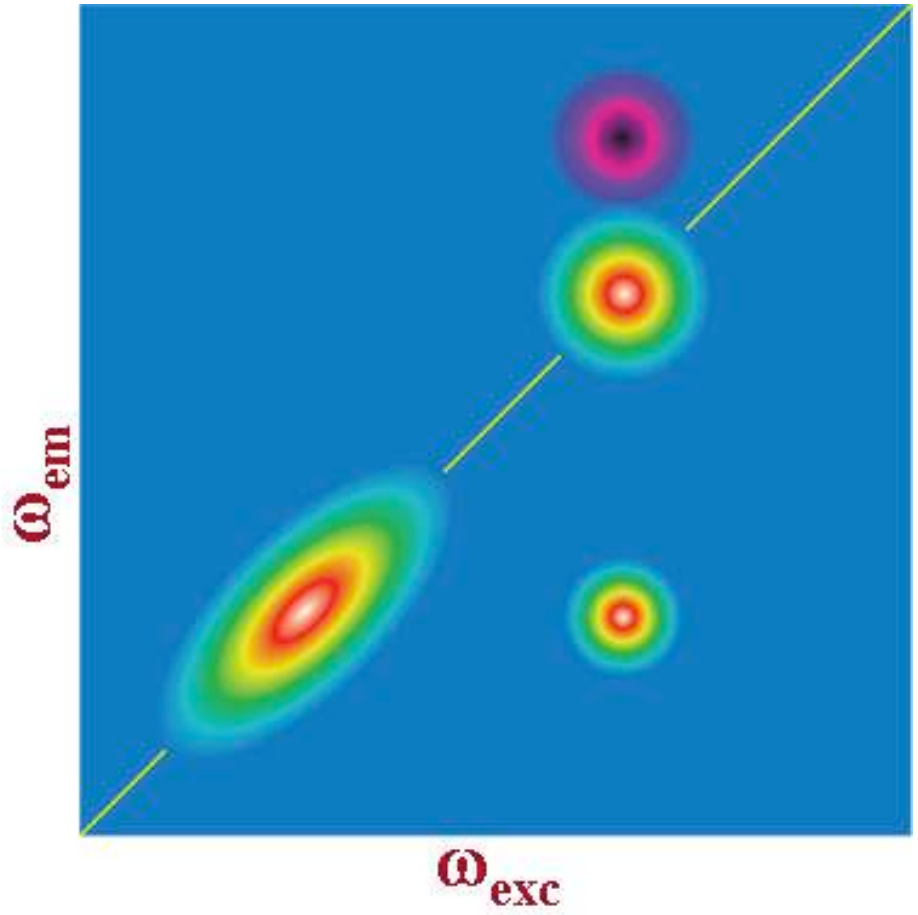

If we integrate the 2D map along the ω_{exc} dimension we obtain a response equivalent to pump-probe

time evolution

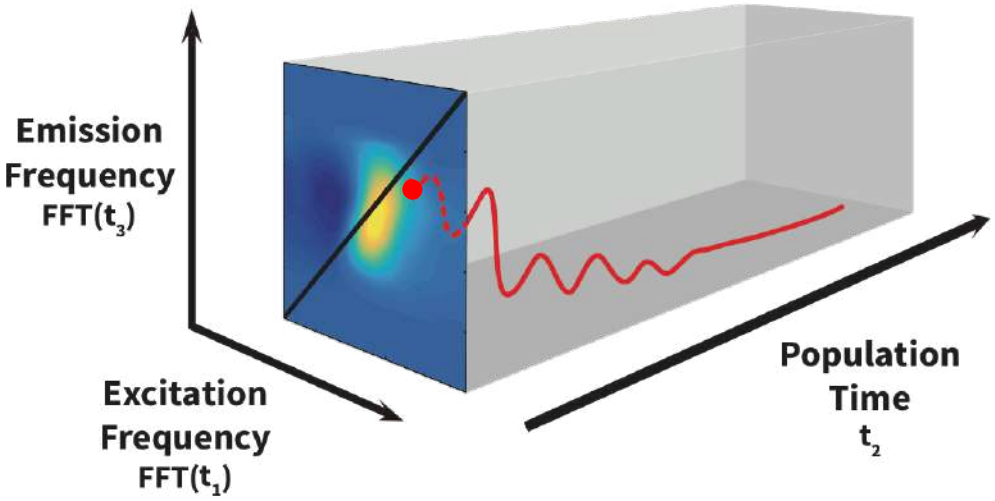

coherence and population dynamics

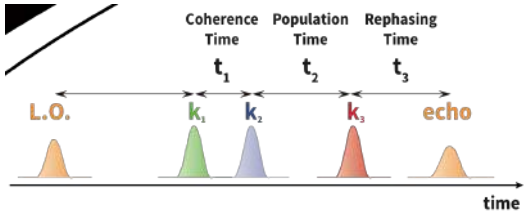

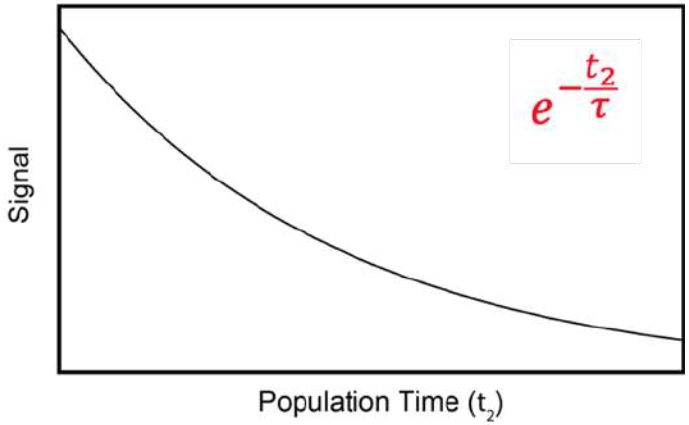

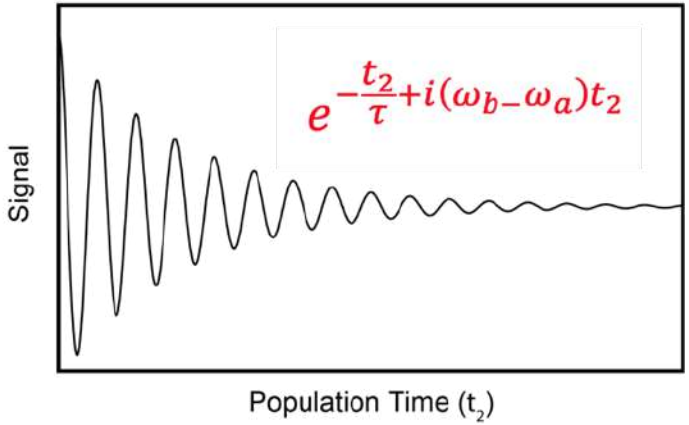

$$\psi(t) = c_a|\psi_a(t)\rangle + c_b|\psi_b(t)\rangle$$

$$= c_a\left|\varphi_a\right\rangle e^{-i\omega_a t} + c_b\left|\varphi_b\right\rangle e^{-i\omega_b t}$$

$$P(t) = |\psi(t)|^2 \propto cos(\omega_a - \omega_b)t$$

OptExp 24 (2016) 24773

3DES

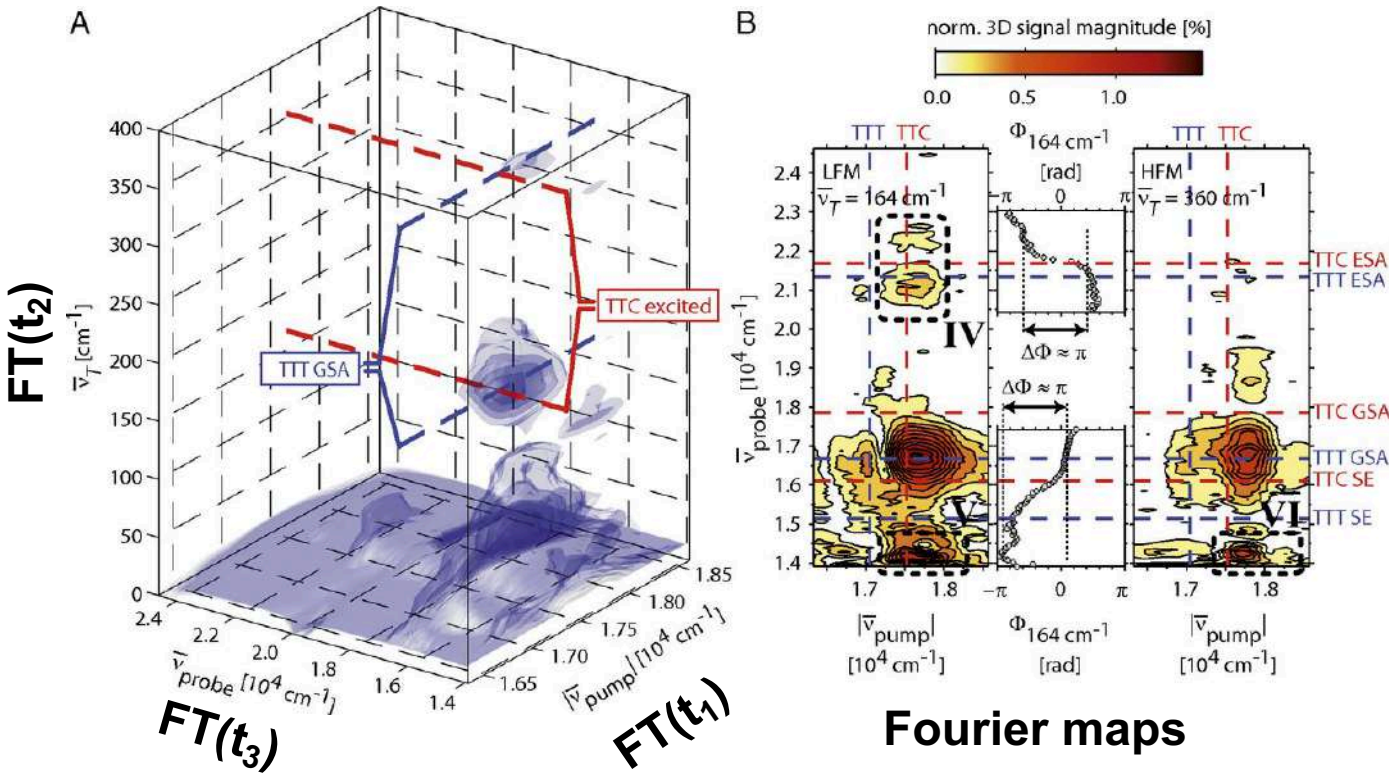

Fourier maps

PNAS 2014, 111 (13)

Fourier maps

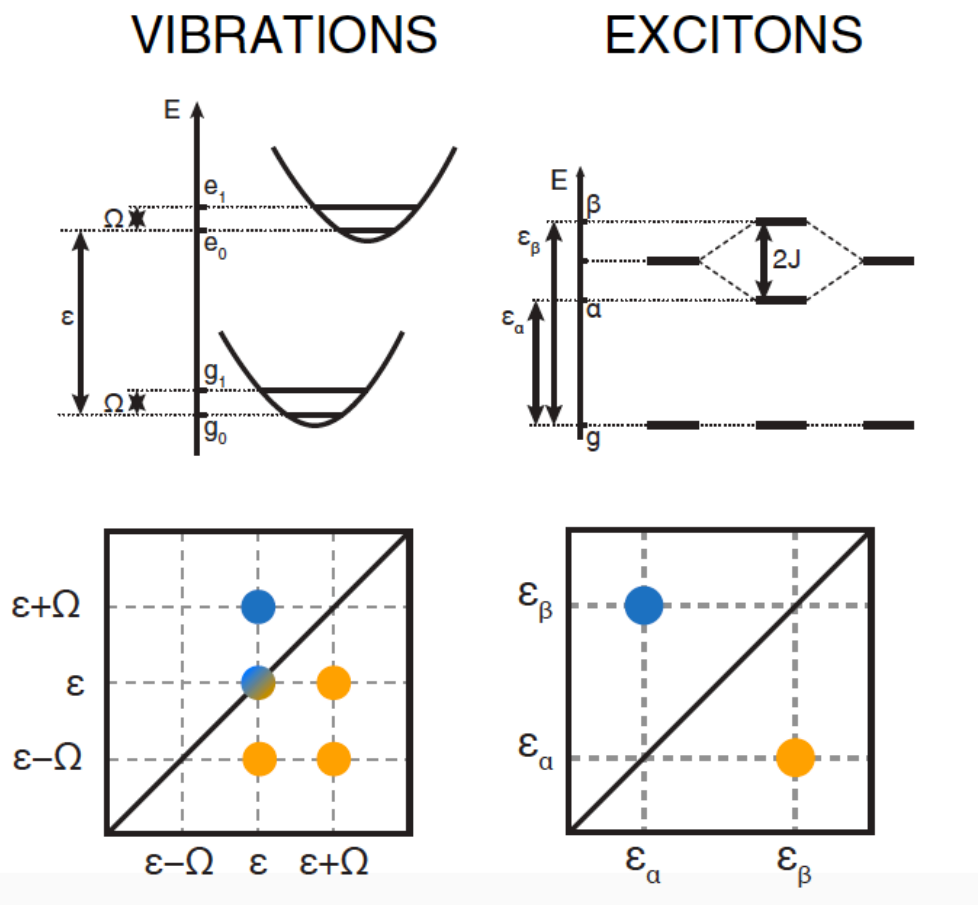

applications: photosynthetic antennas

a fascinating (and still debated!) hypothesis: 'wavelike' EET

nature Vol 446|12 April 2007|doi:10.1038/nature05678

LETTERS

Evidence for wavelike energy transfer through quantum coherence in photosynthetic systems

Gregory S. Engel[1,2], Tessa R. Calhoun[1,2], Elizabeth L. Read[1,2], Tae-Kyu Ahn[1,2], Tomáš Mančal[1,2]†, Yuan-Chung Cheng[1,2], Robert E. Blankenship[3,4] & Graham R. Fleming[1,2]

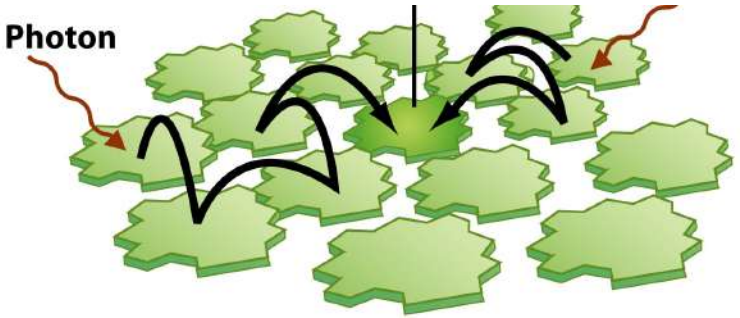

overview of biological antennas

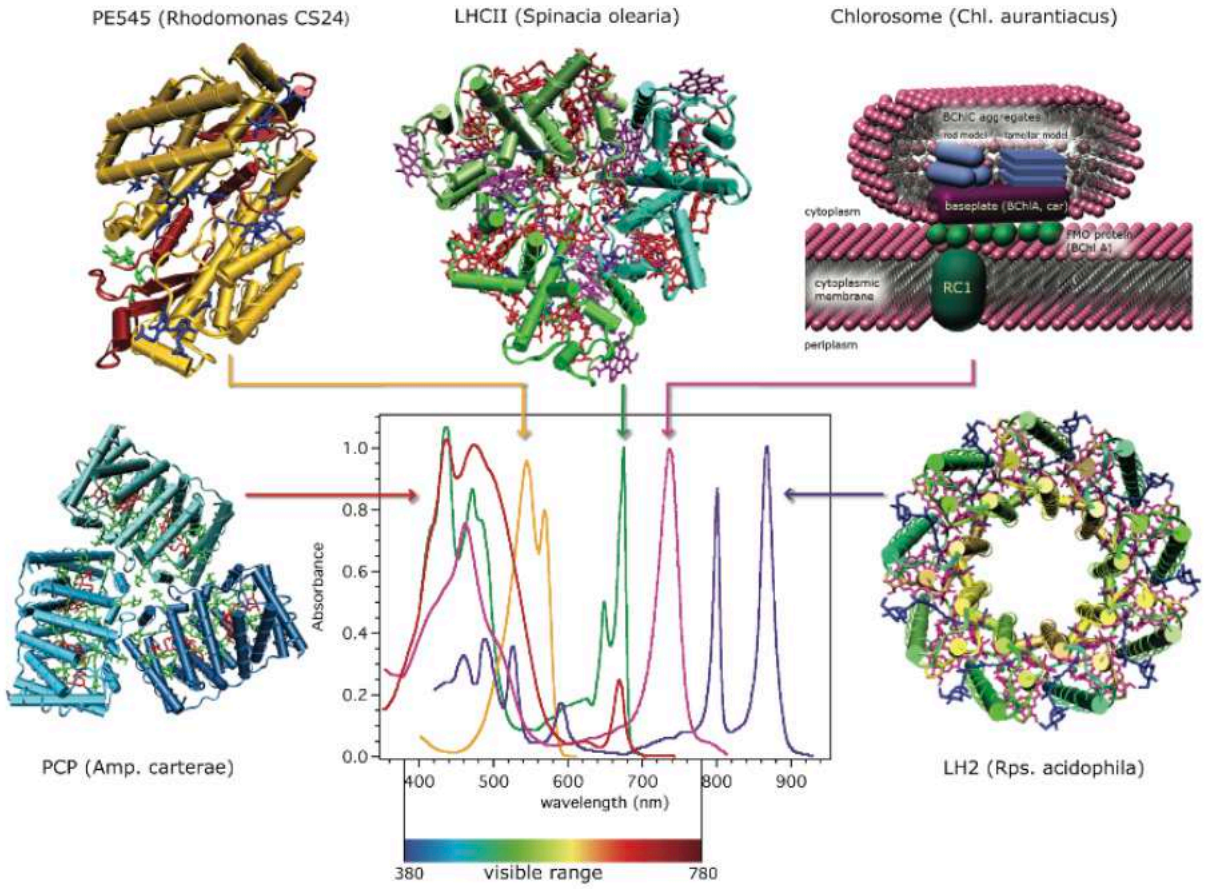

Electronic Energy Transfer in Photosynthetic Antenna Systems, in Energy Transfer Dynamics in Biomaterial Systems, Burghardt, I., May, V., Micha, D.A., Bittner, E.R. (Eds.) 2009

FMO (green sulfur bacteria)

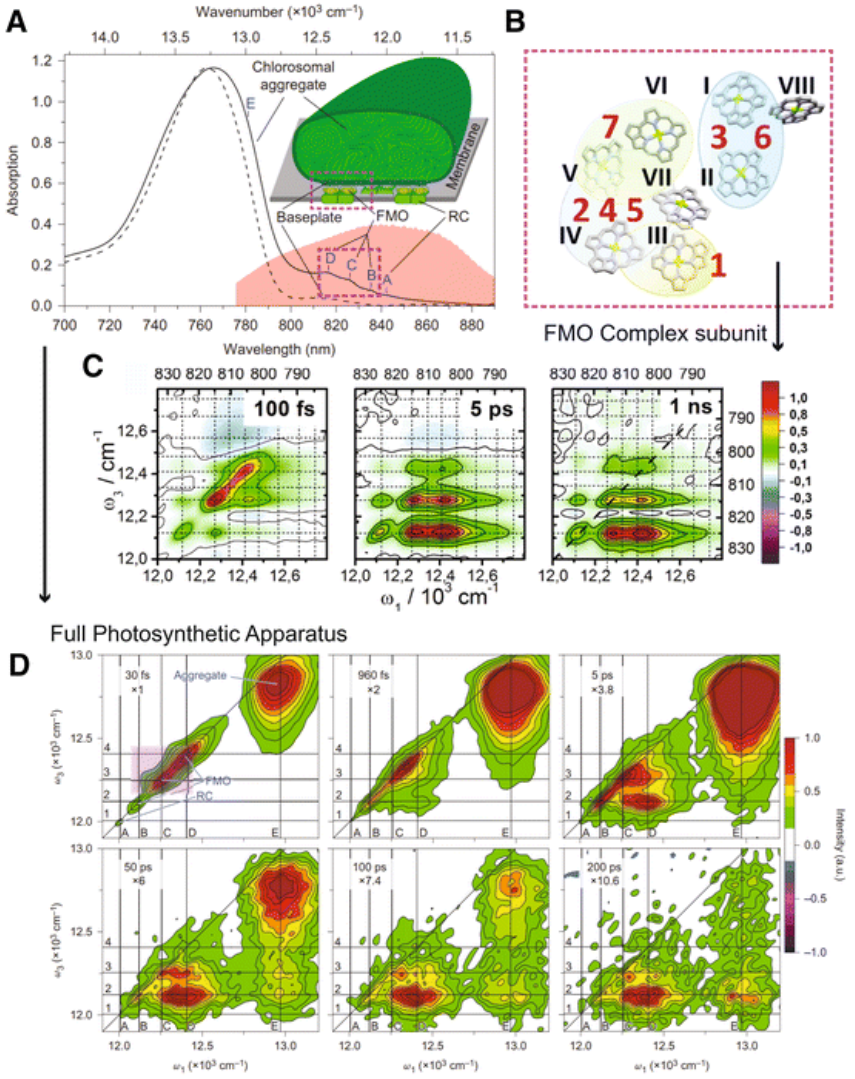

2DES porvided a complete picture on how the energy transfer cascade evolves from the light harvesting antenna complex to the reaction center.

it was possible to track the step-by-step energy flow through the entire unit and observed for the first time that the FMO complex serves as energy conduit between the chlorosome and the RC.

J Phys Chem Lett 7:1653–1660. 2016

LH1 (purple bacteria)

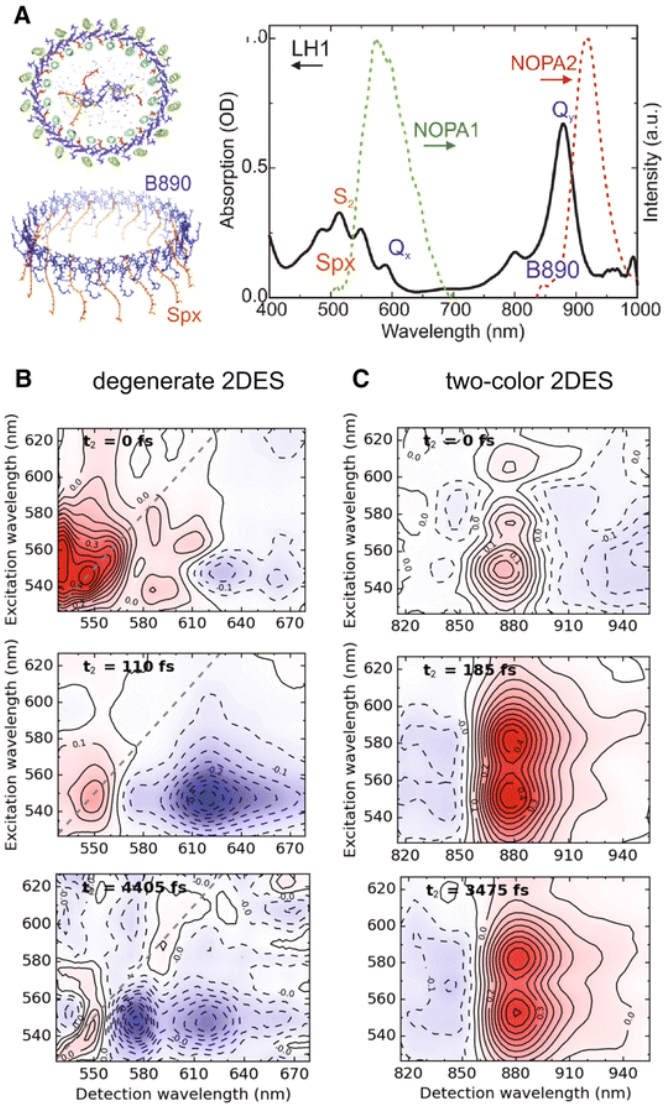

By exciting in the visible range and detecting over both visible and near-IR ranges (2-colors 2DES), it was possible to follow all the photoinduced processes:

i) the Spx internal conversion,
ii) the BChl Qx → Qy internal conversion,
iii) the Spx → B890 EET process

by tracking the formation of several cross-peaks in the 2DES maps.

J Chem Phys 142:212433. 2015

LHCII (green plants)

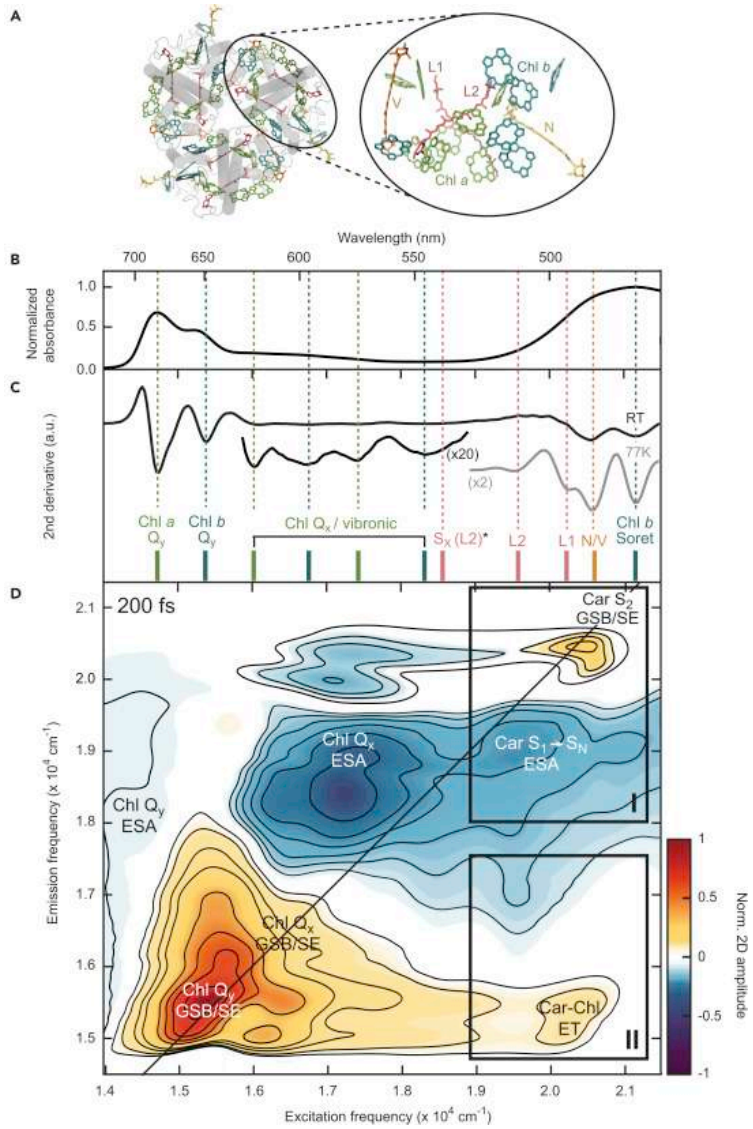

lutein 2 provides a nexus for light harvesting, collecting energy from higher-lying states and funneling it downhill, partially via a debated dark state observed exclusively on lutein 2.

These results show that the protein pocket can tune Car electronic structure via tuning the geometry, a mechanism by which plants control the photophysics of solar energy capture.

Chem 5, 575-584. 2019

PCP (brown algae)

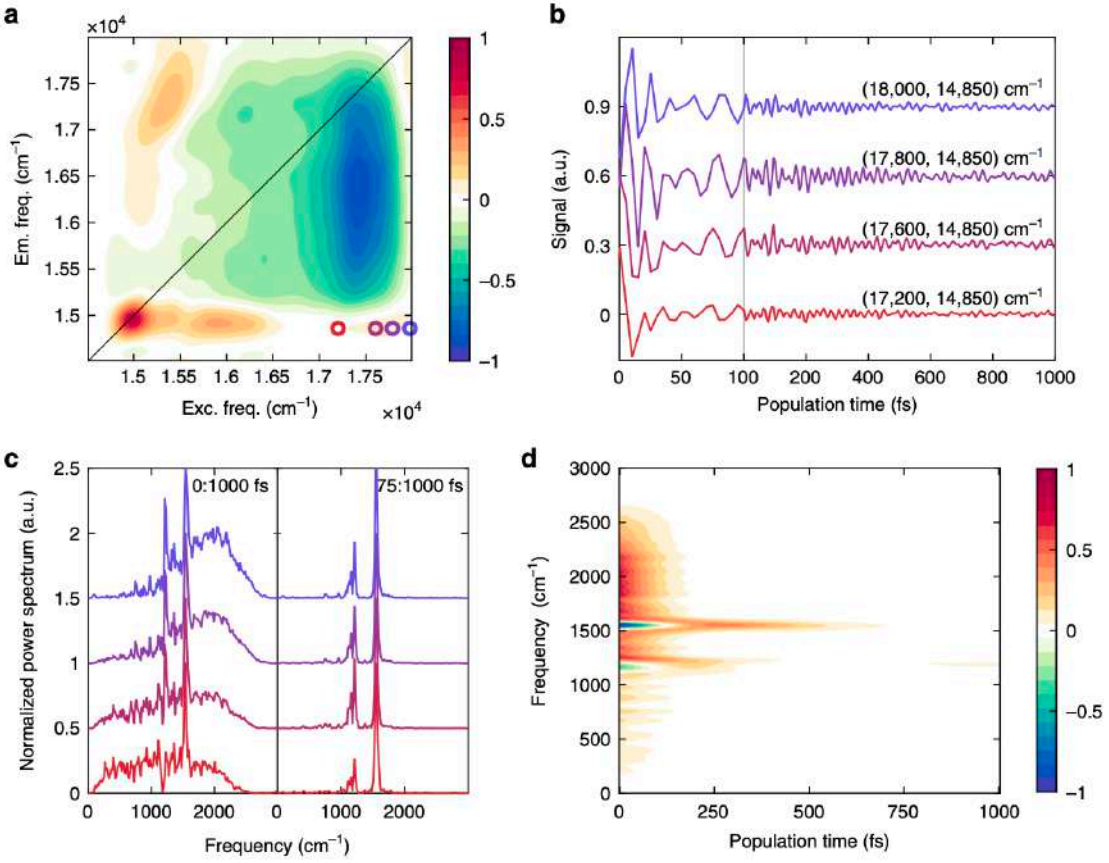

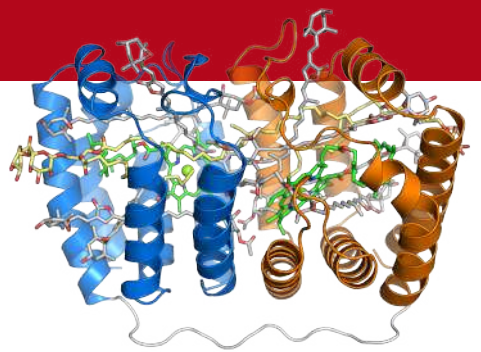

complete mapping of the multiple pathways mechanism of energy flow in PCP, and the relative time constants.

the evolution of the coherence effectively moves the population on the Q_y state: the presence of coherence appears functional to the energy distribution in PCP!

This is important information in current efforts to evaluate possible opportunities to harness coherence to realize, control, and/or drive energy transduction.

NatureComm9(2018)3160

applications: quantum dots

QDs: isolated dots in solution

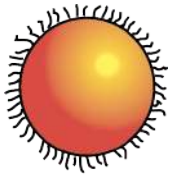

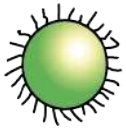

CdSe quantum dots (QDs)

Versatile systems:
photophysical properties tuned modulating size and ligands/solvent

Desired properties:
Stable, processable, dense manifold of states

QDs: relaxation dynamics

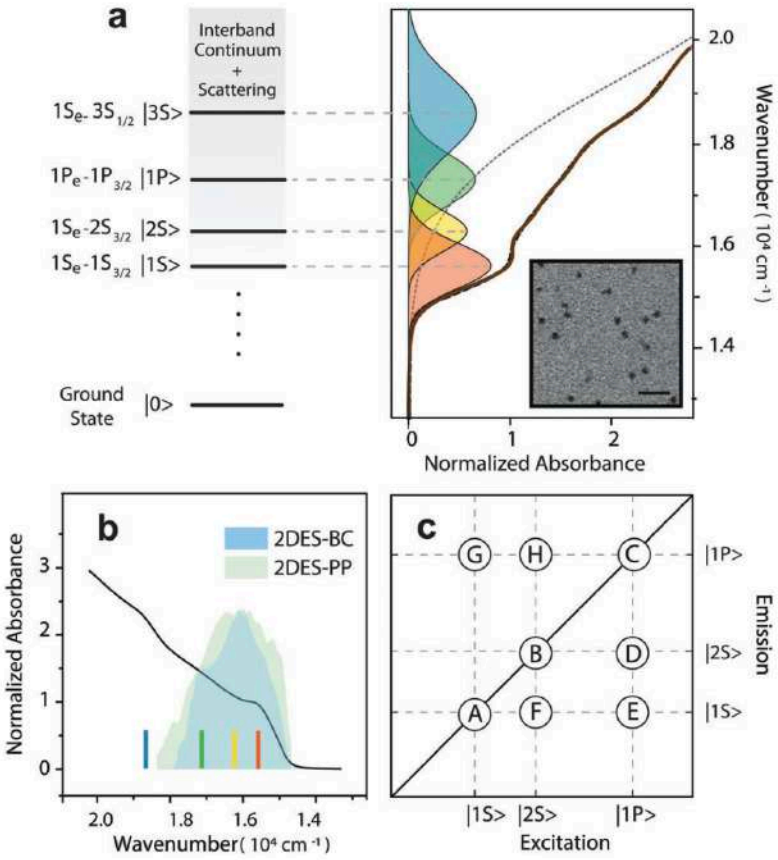

core/shell CdSe/ZnS QDs

« 2D electronic spectroscopy techniques can successfully and efficiently dispel the intertwined dynamics of fast and ultrafast recombination processes in nanomaterials.

Hence, we propose this analysis scheme to be used in future research on novel quantum confined systems »

Phys.Chem.Chem.Phys., 2018, 20, 18176

QDs: coherent evolution

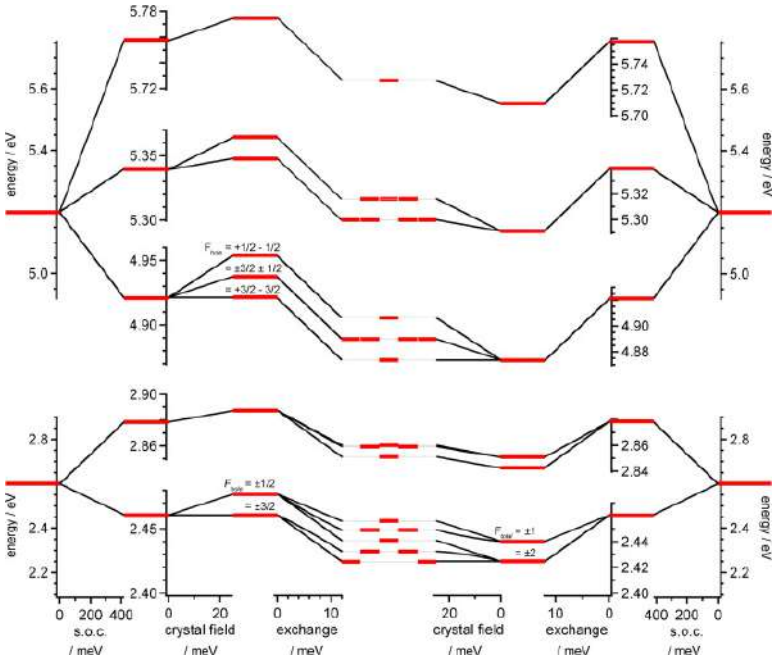

CY Wong et al., J. Luminescence, 131 366-374, 2011

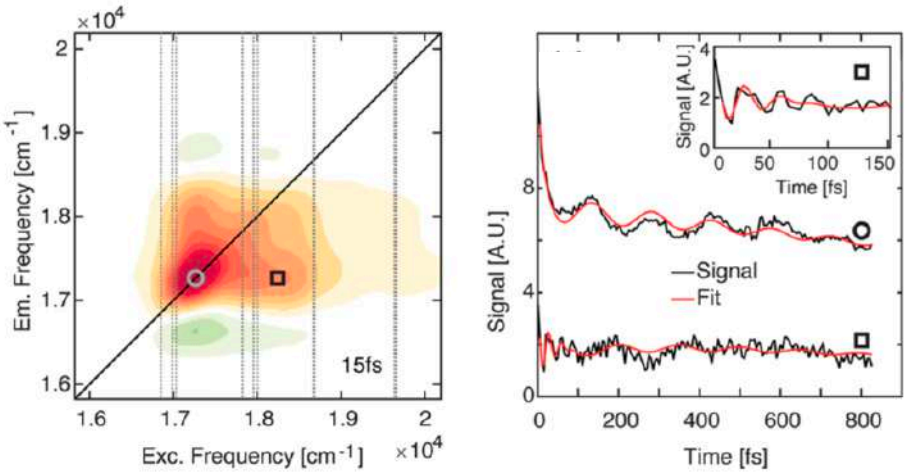

J. Phys. Chem. C 2019, 123, 31286−31293

2DES is sensitive to FINE STRUCTURE of QDs through the detection of the evolution of superposition of electronic states

Signatures of intra-dot coherences evolution

Increasing complexity: QDs dimers

dimers of QDs in solution and solid state. The coupling between dots is modulated through the length of the coupling ligand (di-thiol)

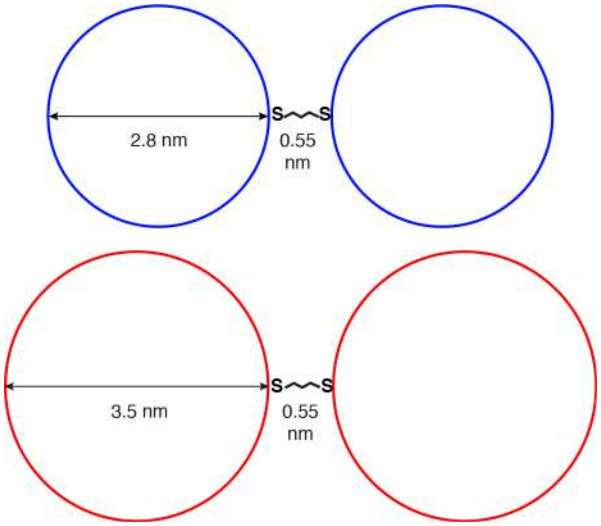

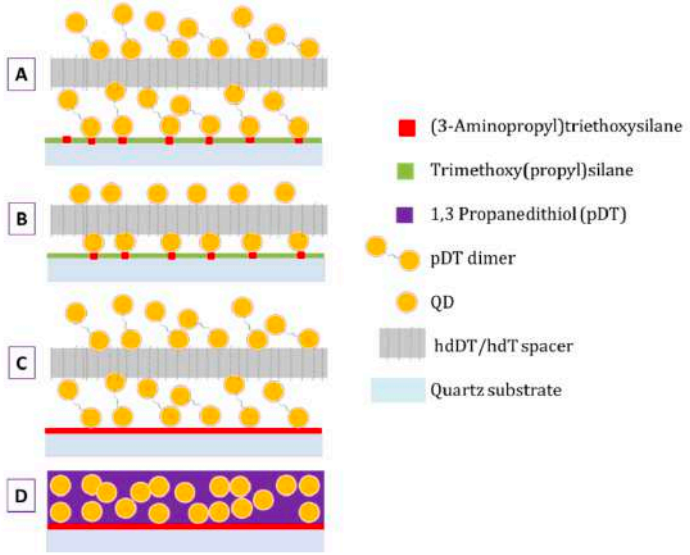

Interest: interacting QDs with delocalized wavefunctions and engineered coherences for applications in quantum technologies

QDs dimers: simulations

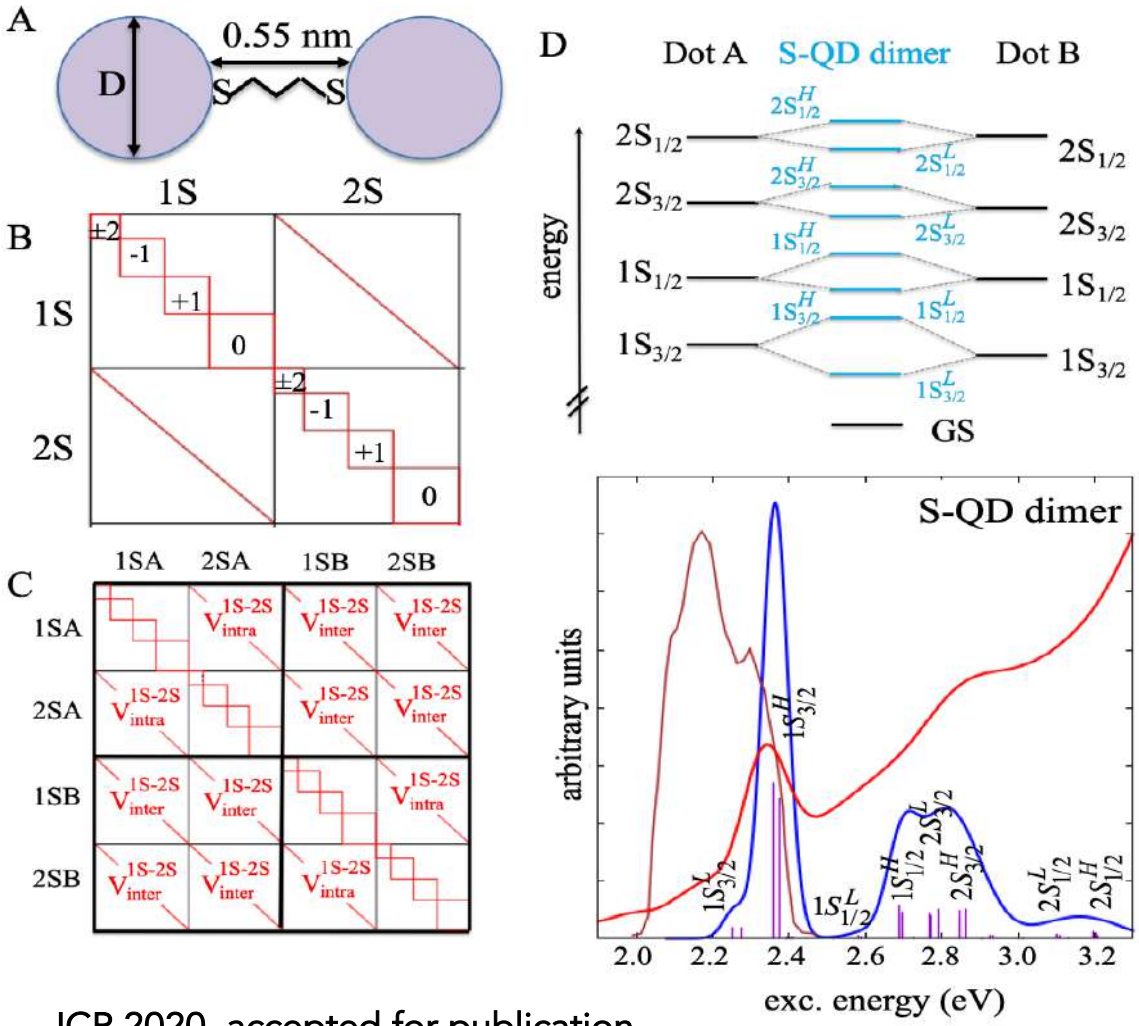

Simulations suggested important guidelines for the design of materials with wanted coherent properties:

- Short distance
- Small size
- Limited size distribution (5% optimal)

JCP 2020, accepted for publication

QDs dimers: inter-dot coherences

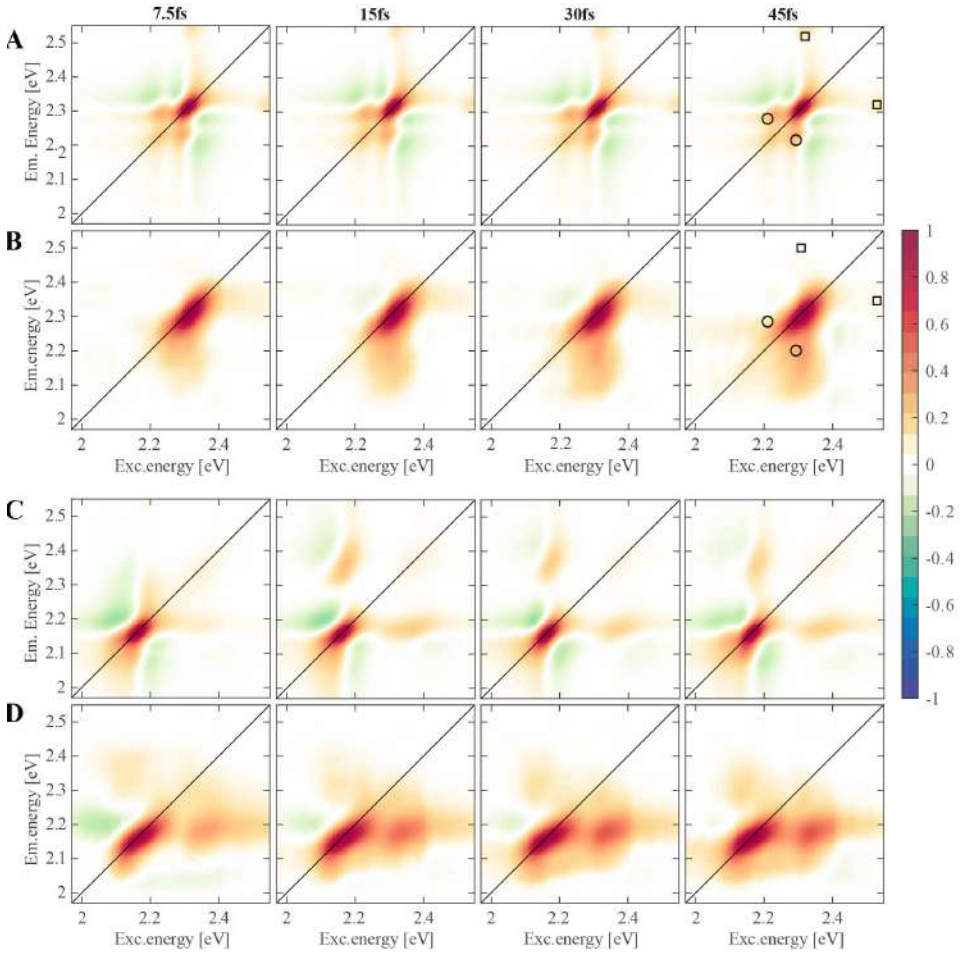

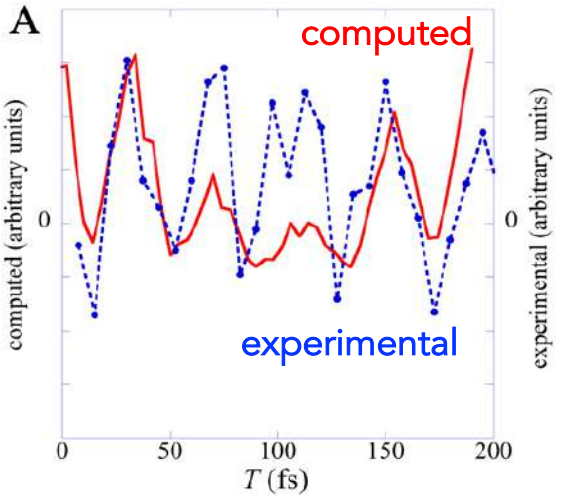

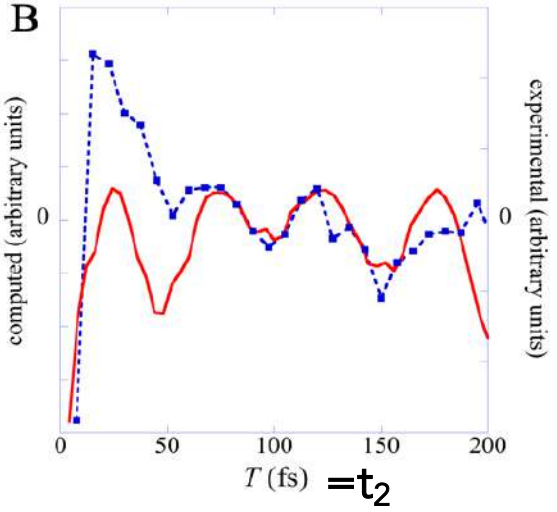

J. Phys. Chem. C 2020, 124, 16222−16231
JCP 2020, accepted for publication

applications: working devices

action-based techniques

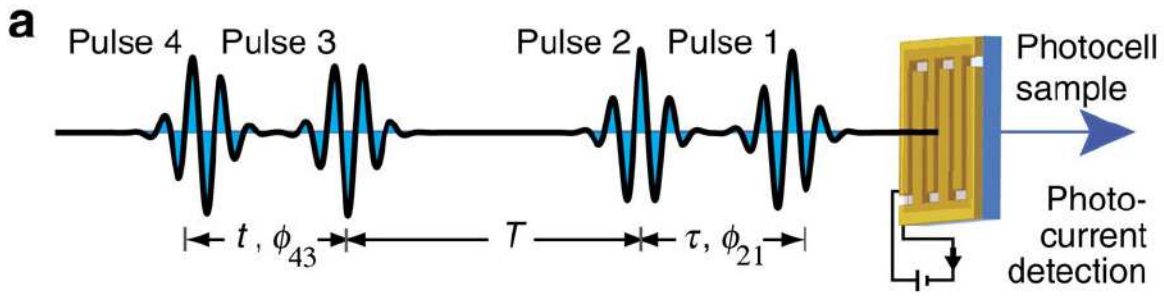

collinear setup (exciting pulses propagate along the same direction)

a fourth pulse is added to the pulse sequence to drive the system into an excited or ground state population.

phase modulation or phase cycling schemes: the phases of the excitation pulses are independently varied by controlled amounts; the excited state population is also modulated, and then it can be read out by some other means, for example, photocurrent or photoluminescence.

Possibility for mass spectrometry detection (and many others detection schemes!) and single molecules implementations

PbS cell

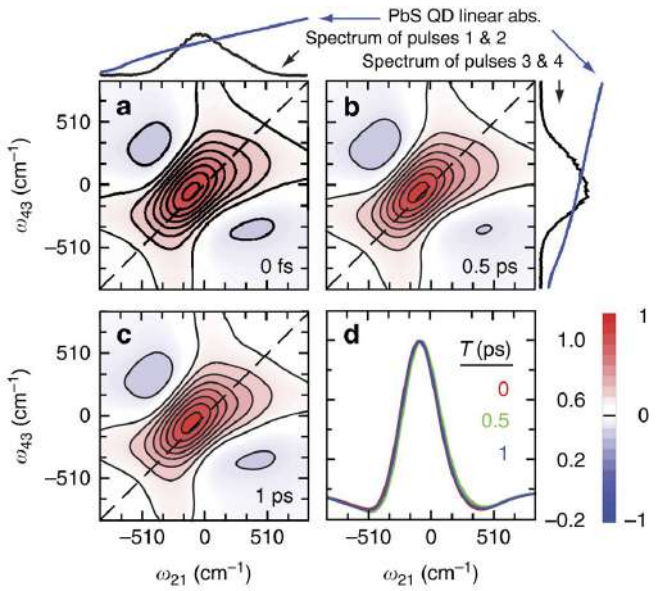

sub-picosecond evolution of two-dimensional spectra consistent with multiple exciton generation

selective spectroscopic information about the coherences and populations that contribute to the final observable, which can be important to understand how and which electronically excited material states are most relevant to the function of an optical or optoelectronic device.

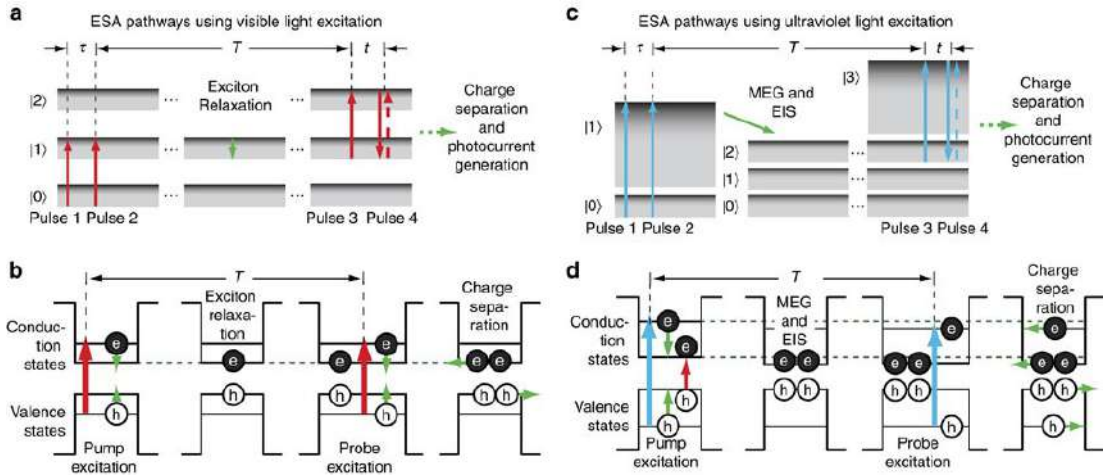

Nature Communications **5**, 5869 (2014)